Journal of
Cardio - Thoracic Medicine

http://jctm.mums.ac.ir

Diabetes, Hypertension, Obesity, and Age as Predictors of Severe COVID-19: A Mathematical Modeling Study

Atena Ghasemabadi [1]*, Somayeh Ghiasi Hafazi [2,3], Habib Allah Esmaeili [4], Maryam Salari [4]

[1] Esfarayen University of Technology, Esfarayen, North Khorasan, Iran.

[2] Department of Biostatistics, School of Health, Mashhad University of Medical Sciences, Mashhad, Iran.

[3] Department of Applied Mathematics, School of Mathematical Sciences, Ferdowsi University of Mashhad, Mashhad, Iran.

[4] Department of Statistics, Faculty of Medicine, Mashhad University of Medical Sciences, Mashhad, Iran.

ARTICLEINFO

Article type:
Original Article

Article history:
Received: 13 May 2026
Accepted: 9 June 2026

Keywords:
COVID-19
Diabetes
Hypertension
Mathematical modeling
Stability analysis

ABSTRACT

Objective: To analyze an epidemiological model of coronavirus disease 2019 (COVID-19) transmission and identify patient characteristics associated with disease severity.

Materials and Methods: An extended SIR-based compartmental model was developed, incorporating asymptomatic/symptomatic classes, hospitalization, intensive care unit (ICU) admission, mortality, reinfection, and environmental transmission. The basic reproduction number R_0) was derived, and stability analysis was performed using Routh-Hurwitz and Castillo-Chavez criteria. Numerical simulations were conducted using MATLAB with data from Mashhad University of Medical Sciences.

Results: The disease-free equilibrium is stable when R_0<1. Clinical findings show: diabetic patients are twice as likely to develop severe symptoms; hypertensive patients have a 3.5-fold higher risk (20% mortality vs. 0.7%); men have seven-fold higher mortality than women; older adults (>40 years) show increased severity; and obese patients (BMI ≥30) have worse outcomes.

Conclusion: R_0 is a critical parameter for disease-free equilibrium stability. Comorbidities (diabetes, hypertension, obesity) and demographic factors (older age, male gender) significantly increase the risk of severe COVID-19 outcomes.

► *Ghasemabadi, A., Ghiasi Hafazi, S., Esmaeili,H.A., Salari, M. Diabetes, Hypertension, Obesity, and Age as Predictors of Severe COVID-19: A Mathematical Modeling Study. J Cardiothorac Med. 2026; 14(2): 1709-1723.* ***Doi : 10.22038/jctm.2026.95622.1529***

Introduction

The severe acute respiratory syndrome coronavirus 2 (SARS-CoV-2), the causative agent of coronavirus disease 2019 (COVID-19), was first identified in Wuhan, China, in late December 2019. The virus's high transmissibility led to its rapid global spread,

* Corresponding author: **Atena Ghasemabadi ,**Esfarayen University of Technology, Esfarayen, North Khorasan, Iran. Tel: 09153523945; E-mail: Ghasemabadi.math@gmail.com & ghasemabadi@esfarayen.ac.ir

prompting the World Health Organization (WHO) to declare a pandemic on March 11, 2020 (1,2). This unprecedented global health crisis has challenged healthcare systems worldwide and necessitated a deep understanding of the disease's transmission dynamics to formulate effective control strategies.

The primary modes of SARS-CoV-2 transmission are respiratory droplets and contact with contaminated surfaces. A critical challenge for healthcare systems has been managing the surge in patients requiring intensive care unit (ICU) admission. In response, governments implemented a range of non-pharmaceutical interventions (NPIs), including lockdowns, social distancing, mask mandates, and case isolation (3,4). The effectiveness of these interventions, however, is highly dependent on public awareness and compliance (5). While crucial for controlling the pandemic, these measures have also imposed substantial economic and social costs (6).

In this context, mathematical modeling has emerged as an indispensable tool for understanding and predicting the trajectory of the pandemic. Early in the pandemic, classic compartmental models, such as the Susceptible-Infected-Recovered (SIR) and Susceptible-Exposed-Infected-Recovered (SEIR) frameworks, were widely used to estimate key epidemiological parameters, including the basic reproduction number (R_0), and to forecast short-term trends (7,8). These models were quickly extended to incorporate more complex and realistic features of COVID-19 transmission. For instance, several studies have highlighted the crucial role of asymptomatic and pre-symptomatic transmission (9). Other research has focused on quantifying the impact of environmental contamination, demonstrating that the virus can persist on surfaces and contribute to transmission, particularly in enclosed settings such as public transport (9,10). Furthermore, a significant body of literature has been dedicated to identifying high-risk populations, consistently showing that age and pre-existing conditions such as diabetes, hypertension, and obesity are major determinants of disease severity and mortality (11).

Numerous mathematical models have been developed to study the transmission dynamics of COVID-19. For instance, Ghasemabadi (12) proposed a model that divides the susceptible population into two groups (those who change their behavior due to fear and those who do not) and the infected population into detected and undetected cases, demonstrating that the disease can be eliminated if the basic reproduction number is reduced below one.

Despite these advancements, many existing models do not simultaneously account for the full spectrum of clinical pathways or the combined effect of demographic and clinical risk factors on patient outcomes. Models often simplify the patient journey by overlooking transitions between stages of care, such as from symptomatic infection to hospitalization and then to ICU admission. Furthermore, while demographic risk factors are well documented empirically, their integration into dynamical models that also account for environmental transmission and waning immunity remains an area requiring further development. To address this gap, we propose a novel compartmental model that extends the classic SIR framework. Our model explicitly incorporates: (i) asymptomatic and symptomatic infectious classes; (ii) a hospitalization class with transfer to an ICU; (iii) disease-induced and natural mortality; (iv) reinfection of recovered individuals; and (v) an environmental pathogen pool that contributes to transmission. This comprehensive structure allows us to simulate the patient journey more realistically and to quantify the impact of key demographic and clinical factors on disease severity and mortality.

The primary contributions of this work are twofold. First, we provide a rigorous mathematical analysis of the proposed model, including the calculation of the basic reproduction number (R_0) and a proof of the local and global asymptotic stability of the disease-free equilibrium. Second, and more importantly from an applied perspective, we calibrate our model using a rich dataset from hospitals affiliated with Mashhad University of Medical Sciences. This allows us, through numerical simulations, to quantify the elevated risks associated with specific patient characteristics. Our findings provide

quantitative evidence that can inform targeted public health strategies and clinical management protocols for high-risk populations, while also contributing to the theoretical foundations of infectious disease modeling.

The remainder of this paper is organized as follows. Section 2 presents the detailed formulation of the mathematical model. We derive the basic reproduction number and analyze the stability of the equilibrium points. A sensitivity analysis of the key parameters is also calculated in this section. The numerical simulations and their biological interpretations are discussed in Section 3. Finally, Sections 4 and 5 conclude the paper with a summary of the findings and their implications for public health.

Materials and Methods

This study developed a mathematical model based on the SIR (Susceptible-Infected-Recovered) framework to simulate the transmission dynamics of SARS-CoV-2 among patients treated in hospitals affiliated with Mashhad University of Medical Sciences. The key hypotheses of the model were as follows: infected individuals were divided into symptomatic and asymptomatic cases; symptomatic patients were admitted to internal medicine wards; severely ill patients were transferred to the ICU; mortality was categorized into natural death and COVID-19-related death (primarily occurring among symptomatic ICU patients); and recovered individuals remained susceptible to reinfection.

The model considered two main transmission pathways: direct transmission from infected individuals (both symptomatic and asymptomatic) and environmental transmission to susceptible individuals. Regarding environmental pathogen dynamics, denoted by (P(t)), the pathogen entered the environment at rates (w_a) (from asymptomatic individuals) and (w_I) (from symptomatic individuals), and left the environment at a rate (w_P). The total population $(N(t))$ in the generalized model was then expressed based on these pathogen dynamics.

$$N(t) = S(t) + A(t) + I(t) + H(t) + K(t) + R(t) + D_1(t) + D_2(t)$$

The transmission dynamics of COVID-19 disease, in general, are shown in Figure 1.
The dynamic model is formulated in the form of Differential Equations :

$$\begin{cases} \frac{dS}{dt} = L - \beta S(t)\big(qA(t) + I(t)\big) - m'S(t) - \beta_p S(t)P(t) + \xi R(t), \\ \frac{dA}{dt} = \beta q S(t)A(t) - \gamma' A(t) - m'A(t) + (1-\alpha)\beta_p S(t)P(t), \\ \frac{dI}{dt} = \beta S(t)I(t) - \varphi I(t) + \alpha\beta_p S(t)P(t), \\ \frac{dH}{dt} = \varphi I(t) - \eta H(t) - UH(t), \\ \frac{dK}{dt} = UH(t) - \theta K(t) - mK(t), \\ \frac{dR}{dt} = \theta K(t) + \eta H(t) + \gamma' A(t) - \xi R(t), \\ \frac{dD_1}{dt} = m'(S(t) + A(t)), \\ \frac{dD_2}{dt} = mK(t), \\ \frac{dP}{dt} = w_a A(t) + w_I I(t) - w_P P(t). \end{cases} \quad (1)$$

The evolution of an individual's life through different stages can be depicted in Figure 1.
The study was conducted by gathering the initial values of state variables and parameters from various valid sources in Table 1. The parameters are constant and non-negative, and are detailed in Table 1.

Basic Reproduction Number

In mathematical epidemiology, the basic reproduction number, denoted by R_0, represents the average number of secondary infections produced by a single primary infected individual during their entire infectious period, when introduced into a completely susceptible host population in the absence of any interventions. Based on the article by (4), R_0can be calculated as follows. For detailed calculations, please refer to Appendix A.

$$R_0 = \frac{\beta S_0 q}{\gamma' + m'} + \frac{(1-\alpha)\beta_p S_0 \omega_a}{(\gamma' + m')\omega_p} + \frac{\beta S_0 \omega_p + \alpha\beta_p S_0 \omega_I}{\varphi\omega_p}.$$

Model Analysis

This section analyzes the local and global asymptotic stability of the disease-free equilibrium point. In mathematical epidemiology, the basic reproduction number (R_0) determines whether an infection will spread or die out. Using standard methods from dynamical systems theory, we analyzed the stability of the

disease-free equilibrium (DFE)—a theoretical state in which no infection exists in the population. To ensure readability for the clinical audience, the mathematical proof of stability (Routh-Hurwitz criterion) and the detailed linearization steps are provided in Appendixes B and C.

Theorem 1 (Local stability): If $R_0 < 11$, the disease-free equilibrium is locally asymptotically stable, meaning that if a small number of infected individuals enters a fully susceptible population, the infection will die out over time. Conversely, if $R_0 > 1$, the DFE is unstable, and an outbreak will occur.

Theorem 2 (Global stability): Using the criterion introduced by Castillo-Chavez and Song (13), we further proved that when $R_0 < 1$, the disease-free equilibrium is globally asymptotically stable. This means that regardless of the initial number of infected individuals (whether small or large), the infection will eventually be eliminated from the population, provided R_0 remains below 1.

These mathematical results confirm R_0 is not merely a theoretical number but a practical threshold for disease control. Public health interventions that reduce R_0 to below 1 (e.g., social distancing, mask-wearing, isolation of infected individuals, environmental disinfection) can guarantee the eventual elimination of COVID-19 from the community, irrespective of how widespread the infection is at the start of the intervention.

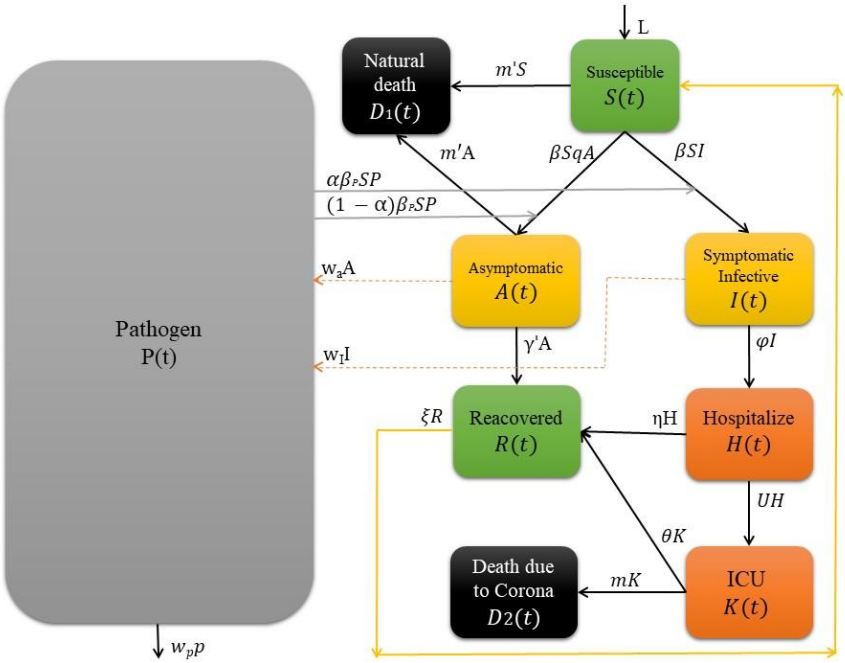

Figure 1. Diagram the model for COVID-19.

Table 1. Interpretation of parameters.

Parameter	Interpretation
L	Birth rate of the human population
β	Infectious contact rate
βp	Rate of transmission from S to A or Idue to contact with P
m	COVID-19-induced death rate
m′	Natural death rate (non-COVID)
θ	Recovery rate of ICU patients
γ′	Recovery rate of asymptomatic individuals
η	Recovery rate of hospitalized (non-ICU) individuals
U	Transfer rate from hospitalization to ICU
ϕ	Transfer rate from symptomatic infection to hospitalization
q	Infectiousness factor of asymptomatic individuals (relative to symptomatic)
α	Rate at which infected individuals become symptomatic
ξ	Reinfection rate of recovered individuals
w_I	Rate of pathogen contribution to the environment by symptomatic individuals
w_a	Rate of pathogen contribution to the environment by asymptomatic individuals

Sensitivity Analysis of the Model

Sensitivity parameters are those that significantly influence the dynamics of a disease. In our system, we have investigated the sensitivity indices of the various parameters.

The normalized forward sensitivity index can be calculated to examine the sensitivity of the basic reproduction number, R_0, to each of its parameters.

$$A_\beta = \frac{\frac{\partial R_0}{R_0}}{\frac{\partial \beta}{\beta}} = \frac{\left(\beta q\varphi + \beta(\gamma' + m')\right) w_p}{L},$$

$$A_{\beta_p} = \frac{\beta_p,(1-\alpha)\, w_a\varphi+\beta_p,\alpha\, w_I\,(\gamma'+m')}{L},$$

$$A_q = \frac{\beta q\, w_p\varphi}{L},$$

$$A_\alpha = \frac{-\alpha\beta_p\, w_a\varphi+\alpha\beta_p\, w_I\,(\gamma'+m')}{L}.$$

$$A_\varphi = \frac{(-\beta\, w_p-\alpha\beta_p\, w_I)\,(\gamma'+m')}{L},$$

$$A_{w_a} = \frac{(1-\alpha)\,\beta_p\, w_a\varphi}{L},$$

$$A_{w_I} = \frac{\alpha\,\beta_p\, w_I(\gamma'+m')}{L},$$

$$A_{w_p} = \frac{-\varphi^2(1-\alpha)\,\beta_p\, w_a-\alpha\,\beta_p\, w_I\,(\gamma'+m')^2}{L\varphi\,(\gamma'+m')},$$

$$A_{\gamma'} = \frac{-\varphi\beta q\gamma' w_p-(1-\alpha)\beta_p w_a\gamma'\varphi}{L(\gamma'+m')},$$

$$A_{m'} = \frac{-\varphi\beta q m' w_p-(1-\alpha)\beta_p w_a m'\varphi}{L(\gamma'+m')},$$

where

$$L = \beta q\varphi\omega_p + (1-\alpha)\beta_p\omega_a\varphi + \left(\beta\omega_p + \alpha\beta_p\omega_I\right)(\gamma' + m').$$

The contact rate (β)refers to the average number of contacts per person per unit of time, indicating how frequently individuals interact with one another. The rate of transmission from S to either A or I due to contact with the pathogen is denoted by β_p. The transmission rates of the pathogen from symptomatic and asymptomatic infected individuals to susceptible individuals (w_I and w_a, respectively) indicate how easily the pathogen can be transmitted and cause infection in a susceptible host. Each of these four factors is directly related to the basic reproduction number (R_0), and an increase in any of them will lead to an increase in (R_0).

In contrast, the natural death rate of the population (m'), the rate at which the pathogen leaves the environment (w_p) , the recovery rate of asymptomatic patients (γ'), and the hospitalization rate of symptomatic patients (φ) all have an inverse relationship with R_0. Increasing any of these factors will result in a decrease in R_0.

The natural death rate (m') represents the rate at which individuals in the population die from causes unrelated to the disease. Increasing this rate would decrease the overall population size, thereby reducing the number of susceptible individuals and leading to a lower R_0.

The rate at which the pathogen leaves the environment (w_p) is the rate at which the virus is removed or inactivated in the surrounding environment. A higher rate of pathogen removal limits the availability of the virus for potential transmission, consequently decreasing R_0.

The recovery rate of asymptomatic patients (γ') is the rate at which asymptomatic individuals recover from the infection and transition to a recovered or immune state. A higher recovery rate means that asymptomatic individuals spend less time in the infectious state, reducing the overall transmission potential and leading to a lower R_0.

The hospitalization rate of patients (φ) represents the rate at which infected individuals require hospitalization. Increasing this rate can reduce the number of individuals actively transmitting the virus in the community, as hospitalized patients are typically isolated and have limited contact with susceptible individuals, resulting in a decrease in R_0.

It is important to note that increasing the natural death rate (m') is neither ethical nor practical as a public health intervention, as it would involve unacceptable actions.

The analysis suggests that focusing efforts on reducing transmission-related parameters, such as the contact rate (β) and the pathogen-mediated transmission rate (β_p), may be a more effective approach than attempting to increase recovery or hospitalization rates. In other words, preventing disease transmission is more effective than relying solely on treatment measures.

Numerical Solutions of the Model

The data related to the population covered by Mashhad University of Medical Sciences

between 2018 and 2019 were extracted from the SINA system. The information related to hospitalizations in the COVID-19 department of the university hospitals in the province was extracted from the Hospital Information System (HIS). This data has the ethics code number 4000330. We have drawn the following diagrams using MATLAB software.

In Figure 2, patients with COVID-19 are categorized into two groups: those with diabetes and those without diabetes. Of these, 7.6% of diabetic individuals developed severe symptoms of COVID-19, while 3.6 % of non-diabetic individuals developed severe symptoms. Diabetic individuals are infected with COVID-19 almost twice as often as non-diabetic individuals (green diagram).

Furthermore, 68% of diabetic individuals experience severe symptoms and require hospitalization, whereas 20% of non-diabetic individuals are hospitalized. The blue graph, which represents hospitalized individuals, consistently increases for diabetics but decreases after 10 months for non-diabetics.

In Figure 3, patients with COVID-19 are categorized into two groups: those with hypertension and those without hypertension. The green graph, which represents individuals with severe symptoms of COVID-19, consistently increases for those with hypertension but consistently decreases for those without hypertension.

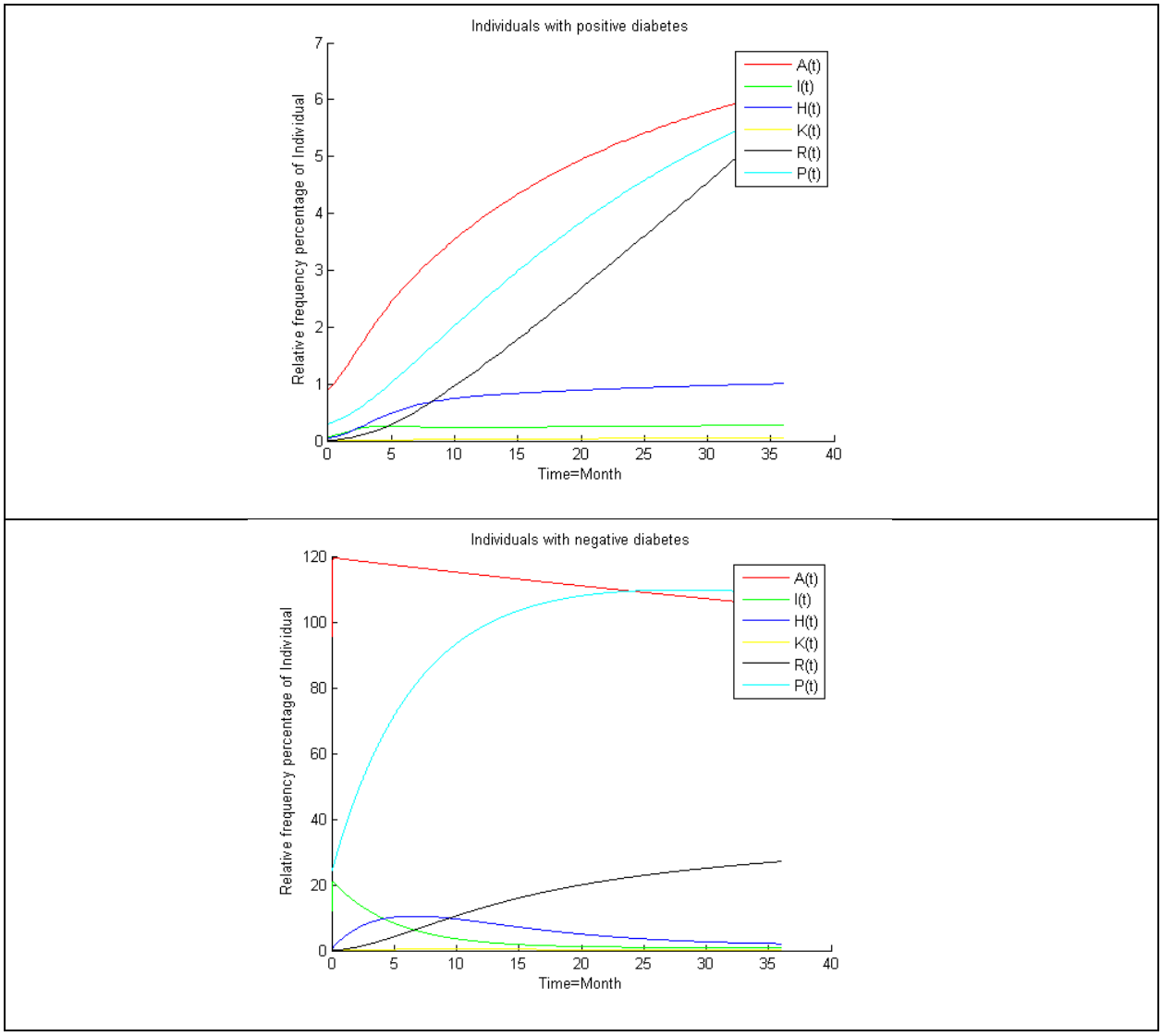

Figure 2. A comparison between COVID-19 patients with positive diabetes and negative diabetes.

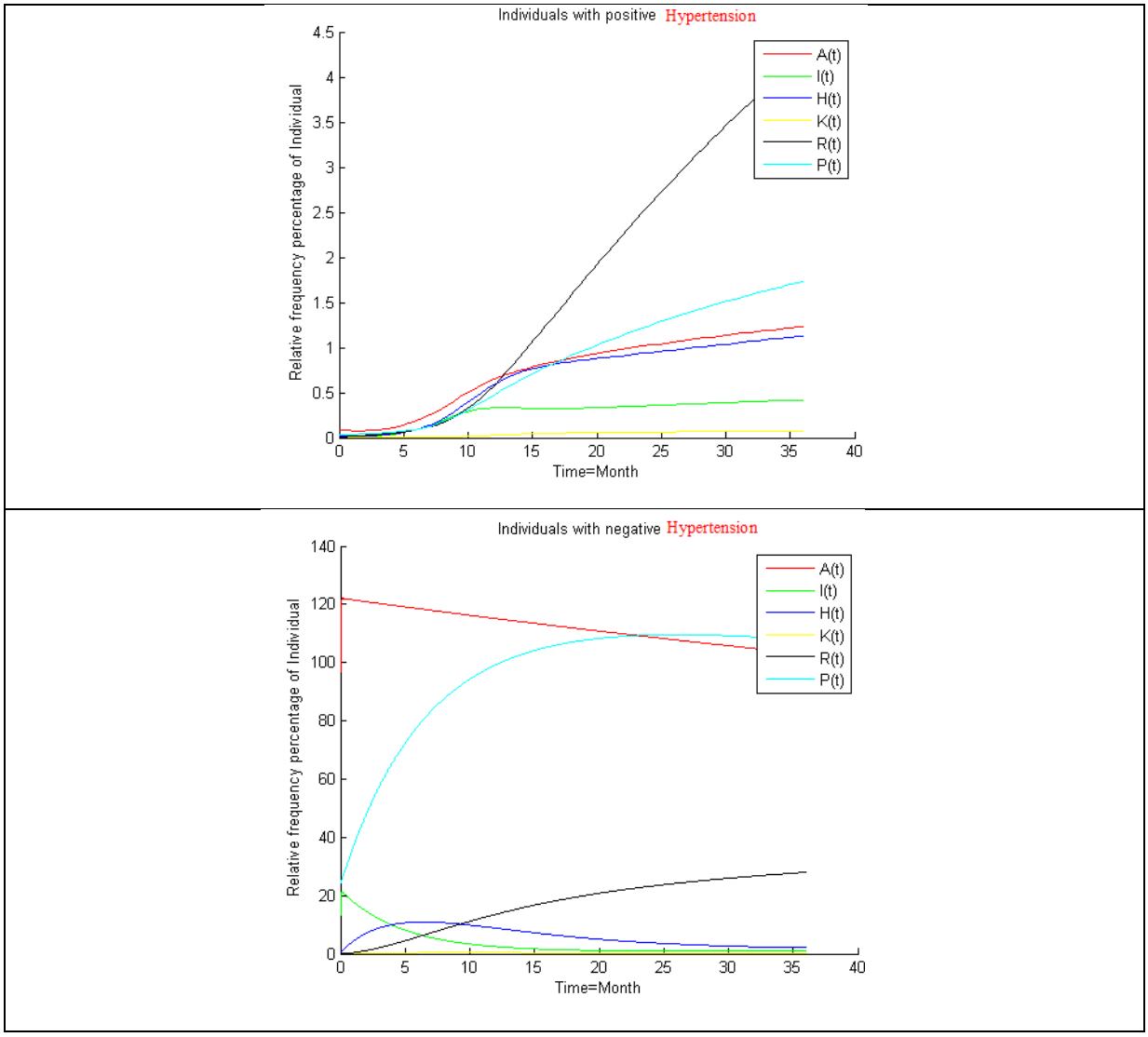

Figure 3. Comparison of the severity of the disease of COVID-19 among men and women.

Specifically, 11% of individuals with hypertension developed severe symptoms of COVID-19, while 3% of individuals without hypertension developed severe symptoms. Thus, individuals with hypertension are almost three and a half times more likely to be infected with COVID-19 and develop severe symptoms (green graph).

Furthermore, 20% of individuals with hypertension die due to COVID-19, whereas 0.7% of individuals without hypertension die due to COVID-19 (coefficient m' in the table).

In Figure 4, patients with COVID-19 are categorized into two groups: male and female. Among those infected with COVID-19 who develop severe symptoms, 29% of men and 18% of women are admitted to the hospital (φ coefficient in the table).

Mortality due to COVID-19 is seven times higher in men than in women (coefficient m' in the table).

The red graph, which represents individuals with mild symptoms of COVID-19, is ascending for women and descending for men. That is, over time, women develop mild symptoms of COVID-19 at an increasing rate, while men show the opposite trend.

Furthermore, 8% of men and 12% of women who are hospitalized with severe symptoms of COVID-19 recover.

In Figure 5, patients with COVID-19 are categorized into four age groups:

- The age group of 31-34 years.
- The age group of 34-37 years.
- The age group of 37-40 years.
- The age group above 40 years.

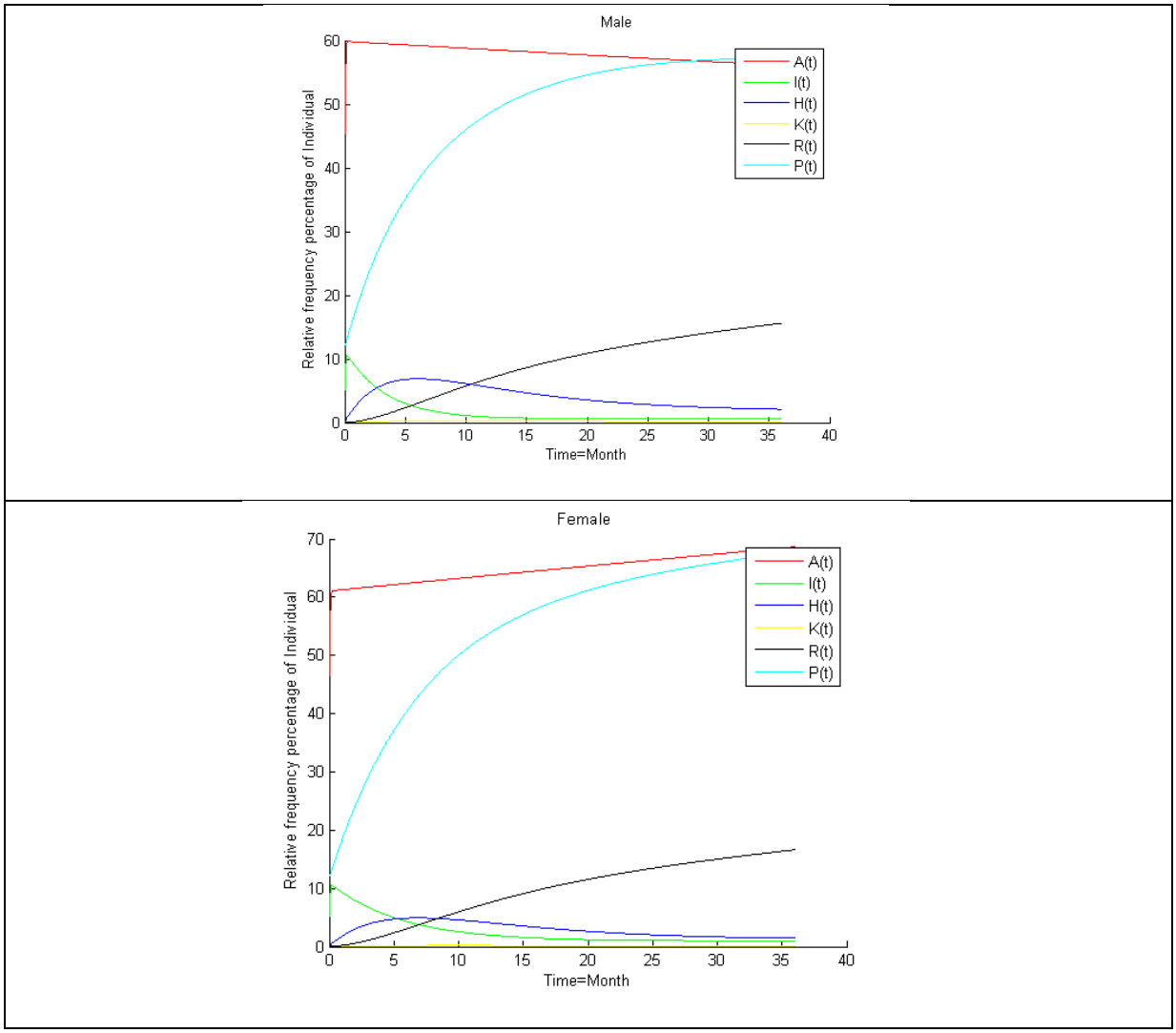

Figure 4. Comparison of severity of COVID-19 disease among men and women.

As shown in Figure 5, the number of hospitalized individuals (blue curves) in all four groups decreases with a slight slope. Consequently, the overall number of hospitalized individuals declines over time until it reaches zero. Additionally, the number of recovered individuals (black curve) shows an upward trend over time in all four age groups, which is a very promising result. The number of individuals admitted to the ICU in all four age groups is close to zero at the beginning of the simulation and tends to zero after a certain period. Finally, the only notable difference among these four graphs is the mortality rate, which in the age group above 40 years shows an upward trend with a steeper slope compared to the other age groups. Such a difference, of course, is not unexpected given the parameters related to these groups.

COVID-19 patients in the age group of 31-34 years are hospitalized less frequently than those in other groups. The red graph, which represents individuals with mild symptoms of COVID-19, shows a significant increase in the age groups of 34 -37 years and above 40 years. COVID-19 patients with severe symptoms in the age group older than 40 years are admitted to the hospital more often than other age groups.

The age group of 31-34 years is admitted to the ICU less frequently than the other groups.

In Figure 6, COVID-19 patients are categorized into three BMI groups:

BMI < 24.9 (normal weight)
BMI < 24.9 (normal weight)
> 25BMI < 29.9 (overweight)
BMI ≥ 30 (obese)

The results show that individuals with BMI < 24.9 develop milder symptoms of COVID-19 compared to the other two groups (red graph).

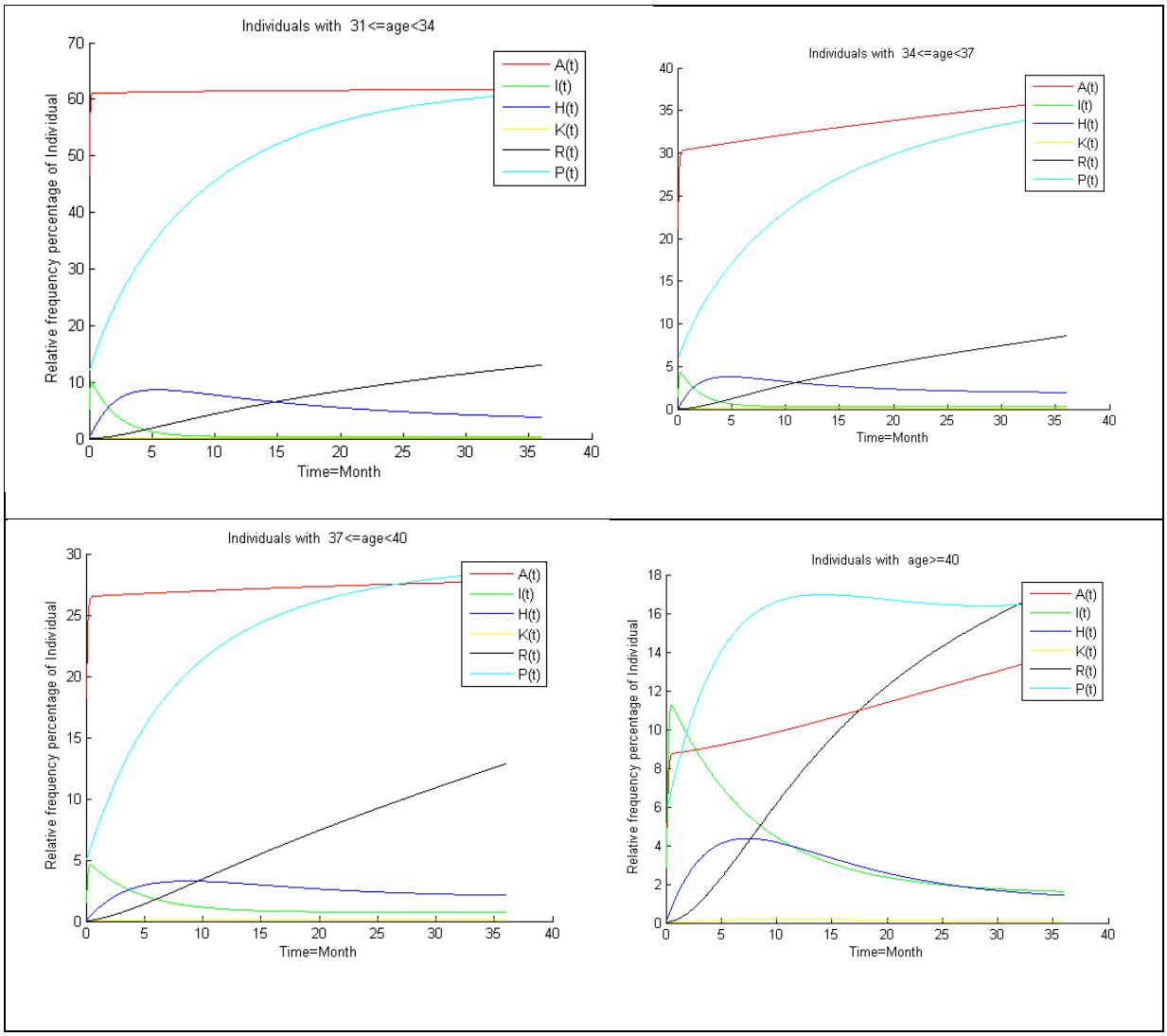

Figure 5. Comparison of the severity of the disease of COVID-19 in different age groups.

The recovery rate of individuals with BMI ≥ 30 is lower than that of the other two groups (black graph). Conversely, the recovery rate of individuals with severe symptoms and BMI < 24.9 is higher than that of the other two groups (black graph).

Furthermore, individuals with BMI ≥30 are hospitalized and admitted to the ICU more frequently than those in the other two groups (coefficients varphi and U in the table).

Results

This study examines the relationship between various patient characteristics and the severity of COVID-19 illness. The data is presented in a series of six figures that categorize COVID-19 patients into different groups based on factors such as diabetes, hypertension, gender, age, and body mass index (BMI).

The key findings include:

Diabetic patients were almost twice as likely to be infected with severe COVID-19 symptoms compared to non-diabetic patients. Diabetic patients also had much higher hospitalization rates.

Patients with hypertension were 3.5 times more likely to develop severe COVID-19 symptoms and had a 20% mortality rate compared to 0.7 % for those without hypertension.

Men were 7 times more likely to die from COVID-19 than women, though women showed increases in mild symptoms over time.

Older age groups, especially those over 40, experienced higher rates of severe symptoms, hospitalization, and mortality compared to younger age groups.

Patients with a BMI over 30 had worse outcomes, including higher rates of hospitalization, ICU admission, and lower recovery rates, compared to those with a lower BMI.

These results highlight the elevated risks faced by patients with certain underlying health conditions and demographics when infected with COVID-19. The findings can inform public health strategies and clinical management for high-risk populations.

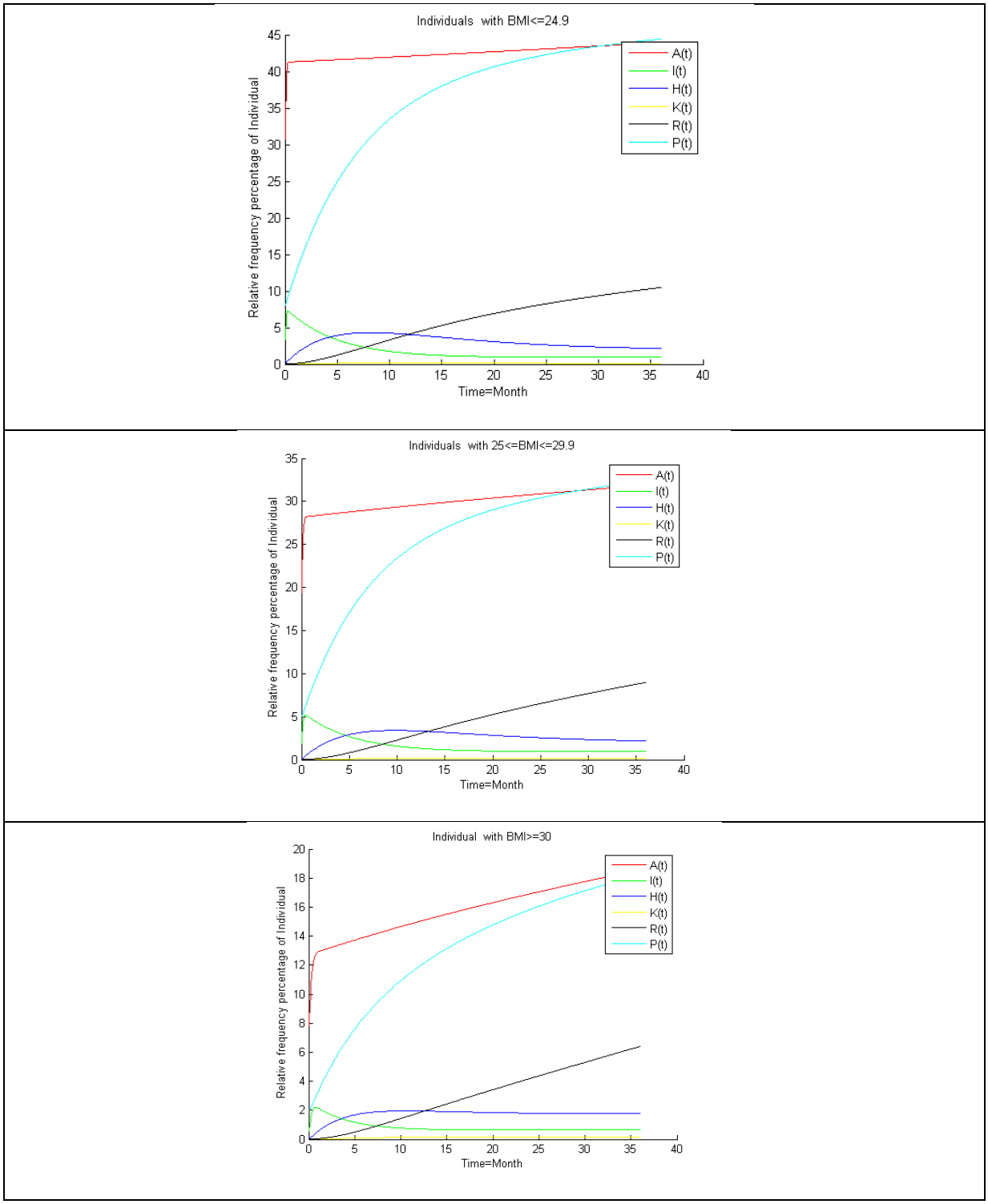

Figure 6. Comparison of severity of COVID-19 disease with different BMI.

Discussion

The primary objective of this study was to analyze the transmission dynamics of COVID-19 using an extended compartmental model that incorporates asymptomatic/symptomatic classes, hospitalization, ICU admission, environmental transmission, and reinfection. Our secondary but clinically more important objective was to quantify the association between key patient characteristics (diabetes, hypertension, sex, age, and BMI) and disease severity using real-world data from hospitals affiliated with Mashhad University of Medical Sciences.

Our numerical simulations yielded several clinically relevant findings. First, diabetic patients were almost twice as likely to develop severe COVID-19 compared to non-diabetic individuals (7.6% vs. 3.6%), and 68% of diabetics required hospitalization versus 20% of non-diabetics. Second, hypertensive patients had a 3.5-fold higher risk of severe infection (11% vs. 3%) and a mortality rate of 20% compared to 0.7% in non-hypertensive patients. Third, male sex was associated with a seven-fold higher mortality than females, although females showed a progressive increase in mild symptoms over time. Fourth, patients older than 40 years experienced higher rates of severe symptoms, hospitalization, and mortality compared to younger age groups. Fifth, obese patients (BMI ≥30) had worse outcomes, including higher hospitalization and ICU admission rates and lower recovery rates compared to normal-weight individuals (BMI <24.9).

From a mathematical epidemiology perspective, we derived the basic reproduction number R_0 and demonstrated that the disease-free equilibrium is locally and globally asymptotically stable when $R_0<1$. Sensitivity analysis revealed that the contact rate (β), pathogen-mediated transmission rate (βp), and environmental shedding rates (w_a, wI) are directly proportional to R_0, while recovery rates (γ′), hospitalization rate (ϕ), and pathogen removal rate (wp) are inversely proportional to R_0.

Our findings are consistent with a large body of literature. Wu et al. (2) reported that comorbidities significantly increase COVID-19 severity, with diabetes and hypertension being the most prevalent risk factors. Similarly, Olfatifar et al. (11) analyzed early epidemiological parameters in Iran and identified older age and male sex as independent predictors of mortality. The seven-fold higher mortality in men observed in our study is also in line with global reports showing sex-based differences in immune response and health-seeking behavior. Regarding obesity, our results align with studies demonstrating that BMI ≥30 is associated with higher odds of ICU admission and mechanical ventilation, likely due to mechanical (diaphragmatic restriction), metabolic (chronic inflammation), and thrombotic mechanisms.

Unlike many previous models that simplified the clinical pathway, our model explicitly tracks transitions from symptomatic infection → hospitalization → ICU admission → recovery or death. This structure allows for more accurate simulation of hospital resource utilization. Additionally, while most studies have focused on direct human-to-human transmission, our inclusion of an environmental compartment ($P(t)$) acknowledges the role of fomites and contaminated surfaces, particularly relevant in hospital and public transport settings (6,8).

The Strengths of This Study Include :

(1) use of real-world patient data from the SINA and HIS of Mashhad University of Medical Sciences, (2) a comprehensive compartmental structure incorporating asymptomatic shedding, environmental transmission, reinfection, and full clinical progression, (3) rigorous mathematical stability analysis (Routh-Hurwitz and Castillo-Chavez criteria), and (4) sensitivity analysis identifying which parameters most strongly influence R_0.

Our findings have several actionable implications. First, risk stratification: diabetic, hypertensive, obese, male, and older (>40 years) patients should be prioritized for early PCR testing, antiviral therapy, and hospitalization. Second, resource allocation: hospitals can use our model to predict ICU bed demand based on the prevalence of these risk factors in their catchment population. Third, public health messaging: targeted

campaigns should emphasize that even mild symptoms in patients with diabetes or hypertension warrant prompt medical evaluation. Fourth, non-pharmaceutical interventions: our sensitivity analysis suggests that reducing contact rates (β) and environmental transmission (βp) is more effective than focusing solely on increasing hospitalization rates (ϕ). In practical terms, mask-wearing, hand hygiene, and surface disinfection remain critical, especially in settings serving high-risk populations (e.g., dialysis centers, diabetes clinics).

Finally, from a modeling perspective, our framework can be adapted for future respiratory pandemics by adjusting compartmental parameters to match the specific transmission and severity profile of a novel pathogen.

Conclusion

This study provides quantitative evidence that diabetes, hypertension, obesity, male sex, and age over 40 years significantly increase the risk of severe COVID-19 outcomes. Our extended SIR-based model offers a robust tool for predicting hospital and ICU demand and evaluating intervention strategies. The basic reproduction number R_0 remains the key threshold parameter for disease elimination, and our sensitivity analysis indicates that transmission-reducing interventions are more effective than treatment-focused strategies alone. These findings can inform evidence-based clinical protocols and public health policies to protect high-risk populations during the ongoing pandemic and future respiratory virus outbreaks.

References

1. Ahmadi A, Fadaei Y, Shirani M, Rahmani F. Modeling and forecasting trend of COVID-19 epidemic in Iran until May 13, 2020. Medical Journal of the Islamic Republic of Iran. 2020 Mar 31;34:27.
2. Wu JT, Leung K, Leung GM. Nowcasting and forecasting the potential domestic and international spread of the 2019-nCoV outbreak originating in Wuhan, China: a modelling study. The lancet. 2020 Feb 29;395(10225):689-97.
3. Ngonghala CN, Iboi E, Eikenberry S, Scotch M, MacIntyre CR, Bonds MH, et al. Mathematical assessment of the impact of non-pharmaceutical interventions on curtailing the 2019 novel Coronavirus. Mathematical biosciences. 2020 Jul 1;325:108364.
4. Okuonghae D, Omame A. Analysis of a mathematical model for COVID-19 population dynamics in Lagos, Nigeria. Chaos, Solitons & Fractals. 2020 Oct 1;139:110032.
5. Eikenberry SE, Mancuso M, Iboi E, Phan T, Eikenberry K, Kuang Y, et al. To mask or not to mask: Modeling the potential for face mask use by the general public to curtail the COVID-19 pandemic. Infectious disease modelling. 2020 Jan 1;5:293-308.
6. Perkins TA, España G. Optimal control of the COVID-19 pandemic with non-pharmaceutical interventions. Bulletin of mathematical biology. 2020 Oct 7;82(9):118.
7. Tsay C, Lejarza F, Stadtherr MA, Baldea M. Modeling, state estimation, and optimal control for the US COVID-19 outbreak. Scientific reports. 2020 Jul 1;10(1):10711.
8. Viceconte G, Petrosillo N. COVID-19 R0: Magic number or conundrum?. Infectious disease reports. 2020 Feb 24;12(1):8516.
9. Mwalili S, Kimathi M, Ojiambo V, Gathungu D, Mbogo R. SEIR model for COVID-19 dynamics incorporating the environment and social distancing. BMC research notes. 2020 Jul 23;13(1):352.
10. Mekonen KG, Habtemicheal TG, Balcha SF. Modeling the effect of contaminated objects for the transmission dynamics of COVID-19 pandemic with self protection behavior changes. Results in Applied Mathematics. 2021 Feb 1;9:100134.
11. Olfatifar M, Alali WQ, Houri H, Pourhoseingholi MA, Babaee E, Seifollahi R, et al. Early estimation of the epidemiological parameters of novel coronavirus disease (COVID-2019) outbreak in Iran: 19 Feb-15 March, 2020. Gastroenterology and hepatology from bed to bench. 2020;13(Suppl1):S134.
12. Ghasemabadi A. Mathematical modeling and control of Covid-19. Mathematical Methods in the Applied Sciences. 2024 Aug;47(12):10478-89.
13. Castillo-Chavez C, Song B. Dynamical models of tuberculosis and their applications. Mathematical biosciences and engineering. 2004;1(2):361.

Appendix A

In this Appendix, we derive the numerical value of the basic reproduction number.
We assume that $S(0)= S_0=N(0)$, allowing us to write three equations using linearization.
Through this linearization, the system is divided into distinct compartments. The matrix G represents the new infection terms, while the second matrix, denoted by Z, represents the secondary illness terms, respectively given by:

$$G = \begin{bmatrix} \beta S_0 q & 0 & (1-\alpha)\beta S_0 q \\ 0 & \beta S_0 & \alpha \beta_p S_0 \\ 0 & 0 & 0 \end{bmatrix}$$

and

$$Z = \begin{bmatrix} \gamma' + m' & 0 & 0 \\ 0 & \text{varphi} & 0 \\ -\omega_a & -\omega_I & \omega_p \end{bmatrix}$$

therefore:

$$GZ^{-1} = \begin{bmatrix} \beta S_0 q & 0 & (1-\alpha)\beta_p S_0 \\ 0 & \beta S_0 & \alpha\beta_p S_0 \\ 0 & 0 & 0 \end{bmatrix}$$

$$\begin{bmatrix} \frac{1}{\gamma'+m'} & 0 & 0 \\ 0 & \frac{1}{\varphi} & 0 \\ \frac{\omega_a}{\omega_p(\gamma'+m')} & \frac{\omega_I}{\omega_p\varphi} & \frac{1}{\omega_p} \end{bmatrix}$$

$$= \begin{bmatrix} \frac{\beta S_0 q}{\gamma'+m'} + \frac{(1-\alpha)\beta_p S_0 \omega_a}{\omega_p(\gamma'+m')} & \frac{(1-\alpha)\beta_p S_0 \omega_I}{\omega_p \varphi} & \frac{(1-\alpha)\beta_p S_0}{\omega_p} \\ \frac{\alpha\beta_p S_0 \omega_a}{\omega_p(\gamma'+m')} & \frac{\beta S_0 \omega_p + \alpha\beta_p S_0 \omega_I}{\varphi\omega_p} & \frac{\alpha\beta_p S_0}{\omega_p} \\ 0 & 0 & 0 \end{bmatrix}$$

Thus we have:

$$R_0 = \frac{\beta S_0 q}{\gamma'+m'} + \frac{(1-\alpha)\beta_p S_0 \omega_a}{(\gamma'+m')\omega_p} + \frac{\beta S_0 \omega_p + \alpha\beta_p S_0 \omega_I}{\varphi\omega_p}.$$

Appendix B

The Proof of Theorem1 : The linearization matrix of the model at the free equilibrium point E_0 is:

$$A = \begin{bmatrix} -m' & -\beta S_0 q & -\beta S_0 & 0 & 0 & xi & -\beta_p S_0 \\ 0 & -\beta S_0 q - (\gamma' + m') & 0 & 0 & 0 & 0 & (1-\alpha)\beta_p S_0 \\ 0 & 0 & \beta S_0 - phi & 0 & 0 & 0 & \alpha\beta_p S_0 \\ 0 & 0 & phi & -eta - U & 0 & 0 & 0 \\ 0 & 0 & 0 & U & -theta - m & 0 & 0 \\ 0 & \gamma' & 0 & eta & theta & -xi & 0 \\ 0 & \omega_a & \omega_I & 0 & 0 & 0 & -\omega_p \end{bmatrix}$$

that the roots of the characteristic equation of this matrix are equal to:

$$\lambda_1 = -m', \lambda_2 = -(\theta + m)$$
$$\lambda_3 = -\xi, \lambda_4 = -(\eta + U).$$

Now consider,

$$\lambda^3 + a_1\lambda^2 + a_2\lambda + a_3 = 0$$

where:

$$a_1 = \nu + w_p - \beta S_0 + \varphi,$$
$$a_2 = w_p(\varphi - \beta S_0) - \alpha\beta_p S_0 w_I + \nu(w_p - \beta S_0 + \varphi) + (1-\alpha)w_a\beta_p S_0,$$
$$a_3 = \nu(w_p(\varphi - \beta S_0) - \alpha\beta_p S_0 w_I) - (1-\alpha)\beta_p S_0 w_a(-\beta S_0 + \varphi),$$

and

$$\nu = -\beta S_0 q + \gamma' + m'.$$

Using the Routh-Hurwitz stability criterion, we can demonstrate that the disease-free equilibrium point is locally asymptotically stable. Since the basic reproduction number R_0 is less than 1, and all model parameters lie between 0 and 1, we can conclude that:

$$\frac{\beta S_0 q}{\gamma' + m'} < 1 \Rightarrow \beta S_0 q < \gamma' + m' \Rightarrow \nu > 0$$

and

$$\frac{\beta S_0}{\varphi} \Rightarrow \beta S_0 < \varphi \Rightarrow a_1 > 0,$$

therefore, a_1 is greater than zero.

Also we have:

$$\frac{\beta S_0}{\varphi} + \frac{\alpha\beta_p S_0 w_I}{\varphi w_p} < 1 \Rightarrow w_p(\varphi - \beta S_0) - \alpha\beta_p S_0 w_I > 0$$

therefore, $a_2 > 0$.

More ever:

$$\frac{\beta S_0 q}{\gamma' + m'} + \frac{\beta S_0}{\varphi} + \frac{(1-\alpha)\beta_p S_0 w_a}{(\gamma' + m')w_p} + \frac{w_I\alpha\beta_p S_0}{\varphi w_p} < 1 \Rightarrow a_3 > 0.$$

Also: $\triangle_2 = \det\begin{bmatrix} a_1 & 1 \\ a_3 & a_2 \end{bmatrix} = a_1a_2 - a_3 = \nu(-\beta S_0 + \varphi)(w_p - \beta S_0 + \varphi) + (\nu + w_p)(-\beta S_0 q + \gamma' + m')(w_p - \beta S_0 + \varphi) - (\nu + w_p)(1 - \alpha\beta_p S_0 w_a)$,

so:

$$\frac{\beta S_0 q}{\gamma' + m'} + \frac{(1-\alpha)\beta_p S_0 w_a}{(\gamma' + m')w_p} < 1 \Rightarrow (1-\alpha)\beta_p S_0 w_a + \beta S_0 q w_p < (\gamma' + m')w_p,$$
$$\frac{\beta S_0}{\varphi} + \frac{\beta S_0 q}{\gamma' + m'} \leq 1 \Rightarrow \beta S_0 q\varphi + \beta S_0(\gamma' + m') \leq \varphi(\gamma' + m'),$$

therefor $\triangle_3 > 0$. $\triangle_3$ is obtained from the following relationship:

$$\triangle_3 = \begin{bmatrix} a_1 & 1 & 0 \\ a_3 & a_2 & a_1 \\ 0 & 0 & a_3 \end{bmatrix} = a_3(a_1a_2 - a_3).$$

Since $a_3 > 0$ and $\triangle_2 > 0$, it is shown that $\triangle_3 > 0$. Therefore, by applying the Routh-Hurwitz stability criterion, we can conclude that the real parts of the roots are negative. Consequently, the disease-free equilibrium point E_0 is locally asymptotically stable.■

Appendix C

The Proof of Theorem2 : To examine the global stability of the system, we apply the criterion introduced by Castillo-Chavez et al.)3). Following Theorem (3), we rewrite system (1) as follows:

$$X = (S, R), \qquad Z = (A, I, H, K, P),$$

$$F(X, 0) = \begin{bmatrix} \mathrm{L} - \mathrm{m}'\mathrm{S} + \xi\mathrm{R} \\ \xi R \end{bmatrix},$$

$$A = \begin{bmatrix} \beta\mathrm{S}_0\mathrm{q} - (\gamma' + \mathrm{m}') & 0 & 0 & 0 & (1-\alpha)\beta_\mathrm{p}\mathrm{S}_0 \\ 0 & \beta\mathrm{S}_0 - \varphi & 0 & 0 & \alpha\beta_\mathrm{p}\mathrm{S}_0 \\ 0 & \varphi & -\eta - \mathrm{U} & 0 & 0 \\ 0 & 0 & U & -\theta - \mathrm{m} & 0 \\ \omega_\mathrm{a} & \omega_\mathrm{I} & 0 & 0 & -\omega_p \end{bmatrix}$$

and

$$\widehat{\mathrm{G}}(\mathrm{X}, \mathrm{Z}) = \begin{bmatrix} \beta\mathrm{qA(t)}\big(\mathrm{S}_0 - \mathrm{S(t)}\big) + (1-\alpha)\beta_\mathrm{p}\mathrm{P(t)}\big(\mathrm{S}_0 - \mathrm{S(t)}\big) \\ \beta\mathrm{I(t)}\big(\mathrm{S}_0 - \mathrm{S(t)}\big) + \alpha\beta_\mathrm{p}\mathrm{P(t)}\big(\mathrm{S}_0 - \mathrm{S(t)}\big) \\ 0 \\ 0 \\ 0 \end{bmatrix}$$

From the first equation of (1), we have $\dot{S} \leq L - m'S$, and integration yields

$S(t) \leq S(0)\exp(-m't) + \frac{L}{m'}(1 - \exp(-m't)) \leq \max(S(0), \frac{L}{m'})$,

for all $\mathrm{t} \geq 0$.

The equilibrium $X^* = \left(\frac{L}{m'}, 0\right)$ is globally asymptotically stable in $\frac{dX}{dt} = F(X, 0)$; it is clear that $\hat{G}(X, Z) \geq 0$. Hence, E_0 is globally asymptotically stable.■